Published in final edited form as:
Muscle Nerve. 2014 August ; 50(2): 286–289. doi:10.1002/mus.24220.

Improved immunoblotting methods provide critical insights into phenotypic differences between two murine dysferlinopathy models

Amber L. Mueller, B.S.[a], **Patrick F. Desmond, B.S.**[a], **Ru-ching Hsia, Ph.D.**[b], and **Joseph A. Roche, P.T., Ph.D.**[c,*]

[a] University of Maryland School of Medicine. Department of Physiology. 655 W Baltimore St, BRB 5-007, Baltimore, 21201. USA

[b] University of Maryland School of Dentistry. Core Imaging Facility. 660 West Redwood St, Howard Hall Rm 696B, Baltimore, MD 21201. USA

[c] Wayne State University, College of Pharmacy and Health Sciences, Department of Health Care Sciences. 259 Mack Ave, Rm. 2217, Detroit, MI 48201

Abstract

Introduction—We adopted a proteomics-based approach to gain insights into phenotypic differences between A/J and B10.SJL murine dysferlinopathy models.

Methods—We optimized immunoblotting of dysferlin by preparing homogenates of the tibialis anterior (TA) muscle under several different conditions. We compared TA muscles of control, A/J, and B10.SJL mice for levels of dysferlin; dysferlin's partners MG53, annexin-A2 and caveolin-3; and the endoplasmic reticulum (ER) stress marker CHOP. We performed immunoelectron microscopy on control rat TA muscle to determine the precise location of dysferlin.

Results—RIPA buffer and sonication improves immunoblotting of dysferlin. The endoplasmic reticulum (ER) stress marker CHOP is elevated in A/J muscle. Dysferlin is localized mostly to membranes close to the Z-disk that have been reported to be part of the Golgi, ER, and sarcoplasmic reticulum (SR) networks.

Conclusion—ER stress might underlie phenotypic differences between A/J and B10.SJL mice and play a role in human dysferlinopathies.

Keywords

Dysferlin; Immunoblotting; Skeletal muscle; ER stress; Dysferlin binding proteins

[*] Corresponding Author: Dr. Joseph A. Roche, Assistant Professor, Department of Health Care Sciences, College of Pharmacy and Health Sciences, Wayne State University. 259 Mack Ave, Rm. 2217, Detroit, MI 48201. USA. joseph.roche@wayne.edu.

The authors declare no conflicts of interest

INTRODUCTION

Dysferlinopathies are muscle wasting syndromes that result from mutations in the *DYSF* gene that encodes the protein dysferlin [1-3]. The A/J and B10.SJL murine dysferlinopathy models arise from different *dysf* mutations and have distinct phenotypes [4-6]. We adopted a proteomics-based approach using immunoblots to assess whether the phenotypic differences between the 2 murine models can be explained by the presence of small amounts of full-length or truncated dysferlin, alterations in the levels of dysferlin binding partners, or differences in cellular stress markers.

METHODS

We optimized our technique for immunoblot detection of dysferlin by systematically studying different methods of extracting protein from the tibialis anterior (TA) muscles of 2 adult A/WySnJ mice (Suppl. Fig. S1A and Supplemental Methods). We then used our optimized immunoblotting methods to compare muscle from dysferlin-sufficient A/WySnJ mice and dysferlin-deficient A/J and B10.SJL mice (N = 3 animals per strain, male, 3-5 m old) for levels of dysferlin, some dysferlin binding partners, and the ER stress marker CHOP (C/EBP homologous protein).

Since ER stress was elevated in A/J muscle, we employed immunoelectron microscopy with the Hamlet antibody to ascertain if dysferlin was enriched in membranes of the ER and SR in TA muscle from control rats (Sprague-Dawley, N = 2, male, 4 m old) [7].

RESULTS

We tested various methods of tissue homogenization to improve the extraction of dysferlin and reduce background noise in immunoblots (Suppl. Fig. S1A). Samples prepared with RIPA buffer instead of 2% NP-40 alone gave more complete extraction of dysferlin with lower background noise (Suppl. Fig. S1B). Sonicating samples for ~10 s reduced background even further and yielded clear, well defined bands. Centrifuging the sample buffer treated homogenates for 30 s at 13,000 RPM (10,000 × G; 5415 C centrifuge, Eppendorf, Hamburg, Germany) only produced a slight improvement in immunoblot quality. Dipping TA muscles into mineral oil prior to snap freezing (for histological preservation) had no effect on the quality of blots for dysferlin.

Immunoblot labeling of dysferlin using our optimized methods showed discrete and prominent bands at ~230 kDa in A/WySnJ muscle homogenates with both the Romeo (N-terminal epitope) and Hamlet (C-terminal epitope) antibodies (Fig. 1A). When the blots were exposed for an optimal duration (~1 min for Romeo and ~2 min for Hamlet) where no additional bands appeared in control samples, dysferlin could not be detected in A/J and B10.SJL lanes. However, with longer exposures (~ 6 min for Romeo and 45 min for Hamlet), faint bands appeared in the B10.SJL lanes and A/J lanes, with the B10.SJL lanes being more prominent. These data suggest the presence of low levels of full-length dysferlin in B10.SJL muscle, and even lower amounts in A/J muscle. Quantitative analyses performed on the overexposed blots showed that B10.SJL and A/J muscle, respectively have about 20% and 10% of the levels of dysferlin found in control muscle (Fig. 1B). A statistically

significant difference between B10.SJL and A/J was detected with Hamlet ($P = 0.004$), but not Romeo ($P = 0.056$). In the overexposed blots, several additional lower molecular weight bands appeared in the A/WySnJ lanes.

We next studied 3 dysferlin binding partners [8,9]. Our improved methods also worked well for immunoblotting MG53, annexin-A2, and caveolin-3 (Fig. 1C). Quantitative analyses showed no significant differences in the levels of these proteins in either of the dysferlin-deficient strains compared to the dysferlin-sufficient strain (Fig. 1D).

As mutant forms of dysferlin have been implicated in ER stress [10], we studied levels of the ER stress marker CHOP using our optimized methods. Our earlier experiments using NP-40 alone yielded blots with high background noise and vertical streaking. The data suggest that our improved methods result in excellent quality immunoblots of CHOP (Fig. 1E) and that it is elevated ~4-fold in A/J muscle compared to control A/WySnJ muscle (Fig. 1F). Interestingly, CHOP levels varied between each of the 3 B10.SJL lanes, and the mean CHOP levels for B10.SJL were not significantly different from control A/WySnJ muscles.

We finally tested the hypothesis that dysferlin and ER stress might be linked, because dysferlin is enriched in membranes of ER and SR. Fig. 1G-I and Suppl. Figs. S2 and S3 suggest that dysferlin is enriched in internal membranes present close to the Z-disk that are reported to be part of the Golgi, ER, and SR networks [11]. Dysferlin was less frequently associated with the contractile apparatus and the M-band, and it was detected rarely at triad junctions.

DISCUSSION

These studies suggest that the use of RIPA buffer and sonication results in more complete extraction of dysferlin and minimizes background noise in immunoblots. Our methodological modifications are not only suitable for dysferlin, but also work well for immunoblots of GAPDH, MG53, annexin-A2, caveolin-3, and CHOP, suggesting that our protocol can be used universally on muscle tissue, as long as denaturing conditions are not contraindicated. With our improved methods, we demonstrate that phenotypic differences between the A/J and B10.SJL murine dysferlinopathy models might be linked to low levels of dysferlin in B10.SJL muscle and high levels of ER stress present in A/J muscle, but they are not linked to changes in levels of MG53, annexin-A2, or caveolin-3. High levels of ER stress might underlie the massive necrosis, inflammation, and delayed functional recovery that is seen A/J muscle following contraction-induced muscle injury, and the presence of low levels of dysferlin might be responsible for faster recovery in B10.SJL muscle [4]. It is likely that certain dysferlin mutations (example: as in the A/J mouse) induce ER stress, because dysferlin is present normally in membranes associated with the Golgi, ER, and SR networks [10,12,13] and might play a role in protein processing and trafficking [14]. Our endeavor to optimize immunoblotting of dysferlin has thus led to the important finding that ER stress might play a role in dysferlinopathies.

Acknowledgments

This work was funded by a grant to JAR from the Jain Foundation Inc. ALM and JAR designed the study, performed the experiments and wrote the paper. PFD provided important technical advice for the optimization of immunoblots and assisted with the quantitative analyses of the blots. RCH and JAR performed the immunoelectron microscopy studies on dysferlin with excellent technical assistance from Mr. John C. Strong and Ms. Johanna C. Sotires in the Core Imaging Facility, University of Maryland School of Dentistry.

ABBREVIATIONS AND ACRONYMS USED

TA	Tibialis anterior
ER	Endoplasmic reticulum
SR	Sarcoplasmic reticulum
CHOP	C/EBP homologous protein
RIPA buffer	Radioimmunoprecipitation assay buffer
SDS	Sodium dodecyl sulfate
PAGE	Polyacrylamide gel electrophoresis

REFERENCES

1. Bashir R, Britton S, Strachan T, Keers S, Vafiadaki E, Lako M, Richard I, Marchand S, Bourg N, Argov Z, Sadeh M, Mahjneh I, Marconi G, Passos-Bueno MR, Moreira Ede S, Zatz M, Beckmann JS, Bushby K. A gene related to Caenorhabditis elegans spermatogenesis factor fer-1 is mutated in limb-girdle muscular dystrophy type 2B. Nat Genet. 1998; 20(1):37–42. [PubMed: 9731527]
2. Liu J, Aoki M, Illa I, Wu C, Fardeau M, Angelini C, Serrano C, Urtizberea JA, Hentati F, Hamida MB, Bohlega S, Culper EJ, Amato AA, Bossie K, Oeltjen J, Bejaoui K, McKenna-Yasek D, Hosler BA, Schurr E, Arahata K, de Jong PJ, Brown RH Jr. Dysferlin, a novel skeletal muscle gene, is mutated in Miyoshi myopathy and limb girdle muscular dystrophy. Nat Genet. 1998; 20(1):31–36. [PubMed: 9731526]
3. Urtizberea JA, Bassez G, Leturcq F, Nguyen K, Krahn M, Levy N. Dysferlinopathies. Neurol India. 2008; 56(3):289–297. [PubMed: 18974555]
4. Roche JA, Ru LW, Bloch RJ. Distinct effects of contraction-induced injury in vivo on four different murine models of dysferlinopathy. J Biomed Biotechnol. 2012; 2012:134031. [PubMed: 22431915]
5. Bittner RE, Anderson LV, Burkhardt E, Bashir R, Vafiadaki E, Ivanova S, Raffelsberger T, Maerk I, Hoger H, Jung M, Karbasiyan M, Storch M, Lassmann H, Moss JA, Davison K, Harrison R, Bushby KM, Reis A. Dysferlin deletion in SJL mice (SJL-Dysf) defines a natural model for limb girdle muscular dystrophy 2B. Nat Genet. 1999; 23(2):141–142. [PubMed: 10508505]
6. Ho M, Post CM, Donahue LR, Lidov HG, Bronson RT, Goolsby H, Watkins SC, Cox GA, Brown RH Jr. Disruption of muscle membrane and phenotype divergence in two novel mouse models of dysferlin deficiency. Hum Mol Genet. 2004; 13(18):1999–2010. [PubMed: 15254015]
7. Gounon P, Rolland J-P. Modification of Unicryl composition for rapid polymerization at low temperature without alteration of immunocytochemical sensitivity. Micron. 1998; 29(4):293–296. [PubMed: 9744087]
8. Lennon NJ, Kho A, Bacskai BJ, Perlmutter SL, Hyman BT, Brown RH Jr. Dysferlin interacts with annexins A1 and A2 and mediates sarcolemmal wound-healing. J Biol Chem. 2003; 278(50): 50466–50473. [PubMed: 14506282]
9. Cai C, Masumiya H, Weisleder N, Matsuda N, Nishi M, Hwang M, Ko JK, Lin P, Thornton A, Zhao X, Pan Z, Komazaki S, Brotto M, Takeshima H, Ma J. MG53 nucleates assembly of cell membrane repair machinery. Nat Cell Biol. 2009; 11(1):56–64. [PubMed: 19043407]

10. Fujita E, Kouroku Y, Isoai A, Kumagai H, Misutani A, Matsuda C, Hayashi YK, Momoi T. Two endoplasmic reticulum-associated degradation (ERAD) systems for the novel variant of the mutant dysferlin: ubiquitin/proteasome ERAD(I) and autophagy/lysosome ERAD(II). Hum Mol Genet. 2007; 16(6):618–629. [PubMed: 17331981]

11. Kaisto T, Metsikko K. Distribution of the endoplasmic reticulum and its relationship with the sarcoplasmic reticulum in skeletal myofibers. Experimental cell research. 2003; 289(1):47–57. [PubMed: 12941603]

12. Sharma A, Yu C, Leung C, Trane A, Lau M, Utokaparch S, Shaheen F, Sheibani N, Bernatchez P. A new role for the muscle repair protein dysferlin in endothelial cell adhesion and angiogenesis. Arterioscler Thromb Vasc Biol. 2010; 30(11):2196–2204. [PubMed: 20724702]

13. Flix B, de la Torre C, Castillo J, Casal C, Illa I, Gallardo E. Dysferlin interacts with calsequestrin-1, myomesin-2 and dynein in human skeletal muscle. The international journal of biochemistry & cell biology. 2013; 45(8):1927–1938. [PubMed: 23792176]

14. Leung C, Utokaparch S, Sharma A, Yu C, Abraham T, Borchers C, Bernatchez P. Proteomic identification of dysferlin-interacting protein complexes in human vascular endothelium. Biochemical and biophysical research communications. 2011; 415(2):263–269. [PubMed: 22037454]

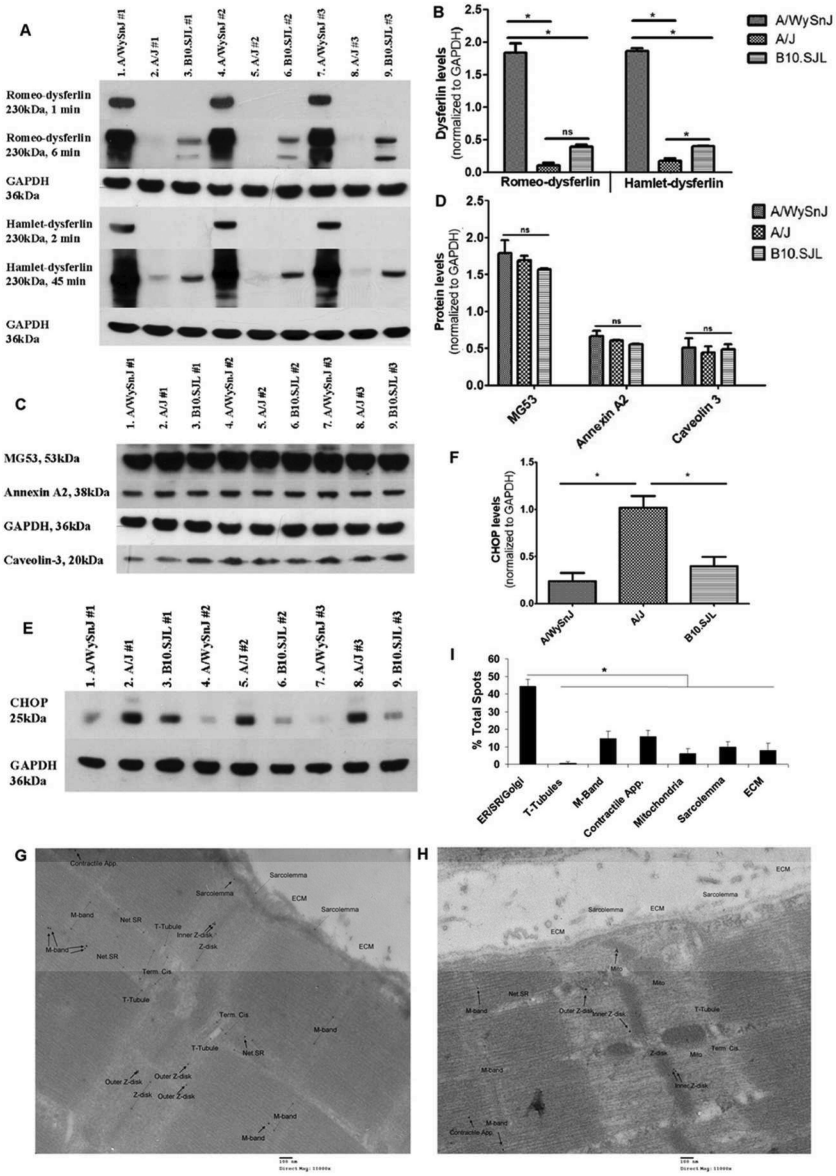

Figure 1. ER Stress is Elevated in Dysferlin-deficient A/J Mouse Muscle

A. Immunoblotting with both Romeo and Hamlet anti-dysferlin antibodies yields discrete bands at ~230 kDa in dysferlin-sufficient A/WySnJ lanes. With longer exposures, faint bands appear in the dysferlin-deficient A/J and B10.SJL lanes with the latter being more prominent. B. Densitometry performed on the ~230 kDa band in the overexposed blots shows a significant difference between A/J and B10.SJL with Hamlet but not Romeo anti-dysferlin (N = 3; Mean ± S.E.M.; *, $P < 0.05$). C-D. Levels of MG53, annexin-A2, and caveolin-3 are not altered in A/J and B10.SJL muscle (N = 3; Mean ± S.E.M). E-F. The ER stress marker CHOP is elevated several-fold in A/J muscle compared to A/WySnJ and B10.SJL muscle (N = 3; Mean ± S.E.M.; *, $P < 0.05$). G-H. Representative images of immunogold labeling of dysferlin in ultrathin sections of TA muscle from 2 rats show that dysferlin is enriched away from the triad junctions in membranes close to the Z-disk that are reported to be part of the ER, SR, and Golgi networks. I. Quantitative analyses suggest that

dysferlin is enriched in components of the ER, SR, and Golgi networks in mature skeletal muscle (Mean ± S.E.M.; *, $P < 0.05$).